ISSN 0020-1685, Inorganic Materials, 2022, Vol. 58, No. 11, pp. 1145–1151. © Pleiades Publishing, Ltd., 2022.
Russian Text © The Author(s), 2022, published in Neorganicheskie Materialy, 2022, Vol. 58, No. 11, pp. 1184–1191.

An X-ray Photoelectron Spectroscopy Study of Ultraviolet Photoannealing-Induced Surface Transformations of Sol–Gel Derived Zinc Oxide-Based Films

A. A. Karmanov[a], I. A. Pronin[a, *], N. D. Yakushova[a], A. S. Komolov[b], and V. A. Moshnikov[c]

[a] *Penza State University, Penza, 440026 Russia*

[b] *St. Petersburg State University, St. Petersburg, 199034 Russia*

[c] *St. Petersburg State Electrotechnical University, St. Petersburg, 197022 Russia*

**e-mail: pronin_i90@mail.ru*

Received April 20, 2022; revised August 14, 2022; accepted September 25, 2022

Abstract—X-ray photoelectron spectroscopy has been used to study structural evolution of zinc oxide synthesized by a sol–gel process adapted to flexible electronics. We assessed the effect of ultraviolet irradiation time on the atomic percentages of different Zn, O, and C species. Increasing the UV treatment time from 90 to 150 min has been shown to considerably reduce zinc concentration in the surface layer, which is accompanied by an increase in the percentage of carbon, predominantly in the form of highly oriented pyrolytic graphite. Photoactivation processes ensure completion of surface structure formation and lead to enrichment of the ZnO surface in oxygen with a binding energy of 531.5 eV, resulting in a zinc-deficient solid solution.

Keywords: zinc oxide, sol–gel processing, UV radiation, structure formation, X-ray photoelectron spectroscopy

DOI: 10.1134/S0020168522110073

INTRODUCTION

There is currently growing interest in research concerned with controlled synthesis of nanomaterials based on wide-band-gap metal oxides for flexible electronics [1]. However, such oxides in the form of thin films are very difficult to use in flexible electronics because stress arising in the material can lead to cracking and splitting at high strain [2]. Zinc oxide, having a band gap of ≈3.3 eV at room temperature [3], is a promising member of this group of nanomaterials. Interest in it is aroused, on the one hand, by its diverse applications in micro- and nanoelectronics [4], gas sensing technologies [5], and photocatalysis [6]. On the other hand, fundamental properties of ZnO are also of importance, including the high exciton binding energy (≈60 meV), high carrier mobility, and good thermal stability [7].

In the context of flexible electronics, zinc oxide has considerable potential owing to not only its possible practical applications, including fabrication of portable sensors and bent displays with a new form factor [8], but also the possibility of controlling its electrical conductivity via surface modification. Note that the problem of degradation of ZnO films can be resolved via synthesis of nanomaterials with a hierarchical spatial organization [9], for example, in the form of a three-dimensional network having a certain degree of bending and stretching/compression. Such a type of structure of nanomaterials is a natural gelation product in sol–gel nanosystems [10]. However, for zinc oxide synthesis high-temperature annealing is needed, which is poorly compatible with the use of flexible low-melting-point polymer substrates.

In connection with this, a sol–gel process was proposed for the preparation of nanostructured ZnO in which the key point is to replace high-temperature annealing by a parallel combination of low-temperature heating and photoannealing under the effect of UV radiation [11]. Note that, even though this approach is viable, specific features of structure formation of zinc oxide and modification of its surface under the effect of UV radiation remain unexplored. Answers to these questions are even more topical in the context of known research dealing with control over the electrical conductivity of ZnO via ultraviolet treatment [12].

In this paper, we report an X-ray photoelectron spectroscopy (XPS) study of surface transformations induced in sol–gel derived zinc oxide-based films by ultraviolet photoannealing in air for various lengths of time.

Table 1. Generalized Zn $2p_{3/2}$ parameters according to the XPS data for the samples differing in UV irradiation time

UV irradiation time, min	Binding energy, eV		
	0	1	2
0	1022.02	1021.93	1022.05
90	1021.91	1021.79	1021.89
150	1021.78	1021.75	1021.94

Before etching (0) and after the first (1) and second (2) etching steps.

EXPERIMENTAL

Synthesis of thin ZnO films with a hierarchical structure. Zinc oxide was synthesized by a technique described previously [11] using a sol–gel process adapted to purposes of flexible electronics. The precursors used for the preparation of film-forming sol were zinc acetate dihydrate ($(CH_3COO)_2Zn{\cdot}2H_2O$), 2-methoxyethanol ($CH_3OCH_2CH_2OH$), and 2-aminoethanol ($HOCH_2CH_2NH_2$), which are well known to have considerable absorption in the UV region, causing changes in chemical bonds. The sol obtained was ripened for 24 h at room temperature. Thin ZnO films were produced by centrifugal casting on oxidized single-crystal silicon substrates ((111) KDB10 boron-doped silicon). The final synthesis step was UV photoannealing in air for 90 and 150 min, which was combined with low-temperature heating (60–200°C). The UV source used for this purpose was a mercury lamp having peak emission wavelengths of 185 and 254 nm. For the low-temperature treatment of the samples, we used a use a flat open heater with a metallic surface.

As reference samples, we used ZnO films prepared from sols with a similar composition by a classic sol–gel synthesis process [13], which were also produced by centrifugal casting and annealed in air for 30 min at a temperature of 550°C.

Characterization of the thin ZnO films with a hierarchical structure. Specific features of structure formation of zinc oxide and modification of its surface under the effect of UV radiation were studied by XPS. XPS spectra were measured under ultrahigh vacuum (~10^{-7} Pa) on an Escalab 250Xi multifunctional photoelectron spectrometer (Thermo Fisher Scientific Inc.) using an AlK_α X-ray source (1486 eV). Survey and core level spectra were taken at an analyzer pass energy of 100 and 50 eV, respectively. In analyzing the measured spectra, we used standard XPS spectra provided by the manufacturer of the spectrometer (Thermo Fisher Scientific Inc.) and took into account reference XPS signal sensitivity factors as described elsewhere [14]. The surface of metal oxides produced in the form of thin films is known to actively adsorb oxygen- and carbon-containing impurities from air [15], so measurements were performed both before and after cleaning the surface with Ar^+ ions. First, Ar^+ ion etching was performed at 500 V for 300 s (first step). Next, the surface was cleaned at 3 kV for 30 s (second step). According to a rough estimate, such cleaning was sufficient to remove about 10 nm of the surface layer.

RESULTS AND DISCUSSION

Survey core level XPS spectra of the ZnO films. Figure 1 shows survey spectra of zinc oxide synthesized using a sol–gel process adapted to purposes of flexible electronics. Spectrum *1* is for a reference sample (sample *1*: ZnO synthesized using high-temperature annealing), and spectra *2* and *3* correspond to the films produced by the described technique at a UV treatment time of 90 (sample *2*) and 150 min (sample *3*). On the whole, the spectra contain characteristic core level peaks of zinc, carbon, and oxygen and Auger peaks, such as Zn *LMM*. Note that the presence of the C 1*s* peak in the spectra can be accounted for by both the presence of residual organic components, incompletely removed from the composition of the sol during annealing, and interaction of the film with the ambient atmosphere. Si signals from the substrate are indistinguishable in the spectra, suggesting that the nanomaterial contains no through pores. It should be especially noted that, in most studies of ZnO, the Zn $2p_{3/2}$ peak (1022.0 eV) was thought to be highly informative. However, the inset in Fig. 1 demonstrates that, in the spectra of the samples under study, this peak shifts only slightly to lower binding energies (≈0.2 eV) with increasing UV irradiation time. This feature of the peak under consideration can be interpreted as evidence of an increase in the number of oxygen vacancies around zinc bonded to oxygen. Surface cleaning of the ZnO films with Ar^+ ions levels down the observed chemical shift, which leads us to conclude that modification occurs predominantly in the surface layer of zinc oxide. Table 1 presents generalized Zn $2p_{3/2}$ parameters for the samples according to the XPS data.

In addition, using the survey spectroscopy results we estimated the percentages of zinc, oxygen, and carbon as functions of UV treatment time before and after surface cleaning. The atomic concentrations of the elements evaluated using peak areas and sensitivity factors are presented in Table 2.

Analysis of the data presented in Table 2 indicates that UV irradiation has a strong effect on the zinc : oxygen atomic ratio in the surface layer of the ZnO

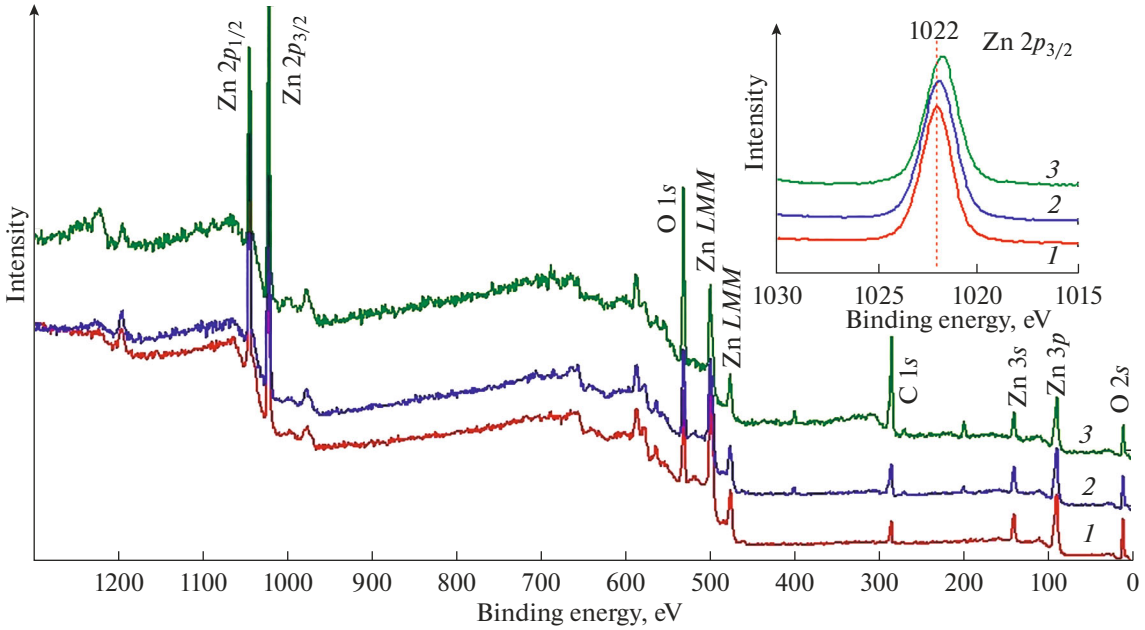

Fig. 1. Survey XPS spectra of the ZnO films: (*1*) high-temperature annealing, (*2*) UV photoannealing for 90 min, (*3*) UV photoannealing for 150 min.

films, which is 0.47 : 0.53 for the reference sample and 0.45 : 0.55 and 0.32 : 0.68 for samples *2* and *3*, respectively. This can be interpreted as deficiency of zinc atoms in the surface layer and/or enrichment in oxygen atoms, resulting in a large nonstoichiometry of the zinc oxide. With allowance for the above-mentioned increase in the number of vacancies in the oxygen sublattice with increasing photoannealing time, accompanied by a change in Zn $2p_{3/2}$ binding energy, analysis of data on stoichiometry evolution leads us to make the following assumptions regarding changes in surface structure: The formation of oxygen vacancies is accompanied by filling of interstitial sites, rather than by oxygen release to the ambient atmosphere. The zinc deficiency in the surface layer is caused by zinc diffusion to the bulk of the material. Relationships between the binding energy, stoichiometry, and structural perfection of zinc oxide were considered in detail by Pronin et al. [16]. Note that two-step Ar^+ ion etching increases the Zn : O ratio, but the percentage of Zn in the irradiated films after etching exceeds that in the unirradiated films (0.62 : 0.38 and 0.68 : 0.32 against 0.58 : 0.42), which cannot be accounted for by just desorption of oxygen-containing adsorbates. In addition, all of the samples are characterized by high carbon content, 25.91, 35.16, and 58.54 at %, which considerably decreases during the cleaning process: to 4.40 and 3.27% in sample *1* and less markedly in samples *2* and *3* after UV treatment for 90 and 150 min. Data on atomic C concentration lead us to conclude that not only does carbon adsorb on ZnO, but it also is located at a depth considerably greater than ≈10 nm; that is, it participates in film structure formation.

Specific features of the O 1*s* core level in the ZnO films. As pointed out above, information about the Zn $2p_{3/2}$ core level is insufficient for detailed analysis of structure formation of zinc oxide in sol–gel nanosystems under UV irradiation. In connection with this, it was reasonable to study the O 1*s* level, which, accord-

Table 2. Atomic compositions according to the XPS data for the samples differing in UV irradiation time

Element	Atomic percent								
	sample *1*			sample *2*			sample *3*		
	0	1	2	0	1	2	0	1	2
Zn	34.91	54.85	56.13	29.15	49.15	50.81	13.24	39.62	51.44
O	39.18	40.75	40.60	35.69	37.80	31.08	28.22	30.90	23.97
C	25.91	4.40	3.27	35.16	13.05	18.11	58.54	29.48	24.59

0, 1, and 2 have the same meaning as in Table 1.

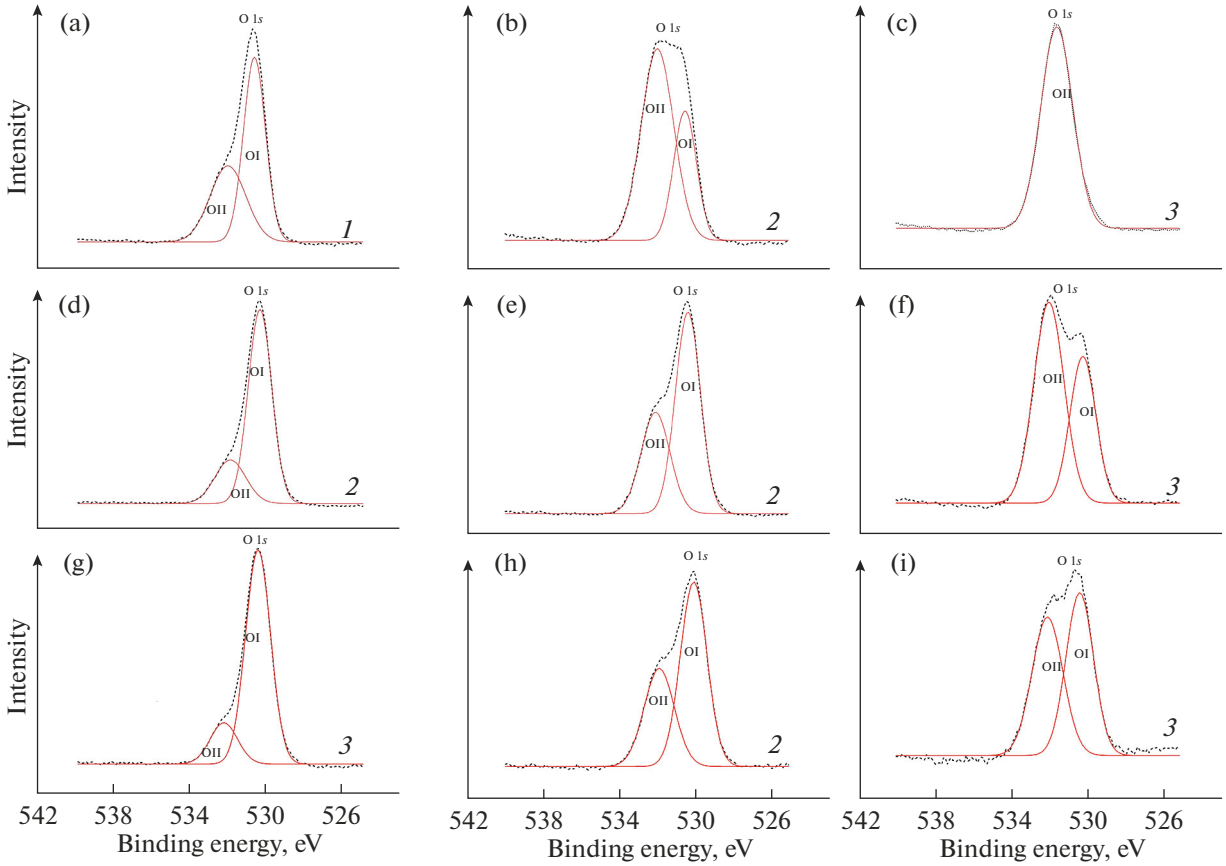

Fig. 2. O 1*s* spectra of the ZnO films produced at various UV photoannealing times: (a, d, g) high-temperature annealing, (b, e, h) UV photoannealing for 90 min, (c, f, i) UV photoannealing for 150 min; (b, e, h) first and (c, f, i) second Ar^+ etching steps.

ing to similar previous studies, provides valuable information regarding not only the stoichiometry of the material but also the density of adsorption centers [17]. Figure 2 shows O 1*s* spectra of the films before and after two-step surface cleaning. The spectra in Figs. 2a–2c correspond to the samples before Ar^+ ion etching; the spectra in Figs. 2d–2f were obtained after the first etching step; and the spectra in Figs. 2g–2i, after the second etching step.

Analysis of these spectra indicates that the O 1*s* signal can be decomposed into components with binding energies of ~530.5 (OI) and ~532.0 eV (OII). Note that the lower energy component corresponds to oxygen in the crystal lattice of ZnO, whereas the higher energy component can arise from both the general lattice oxygen deficiency in the nanomaterial (that is, an O–Zn bond surrounded by oxygen vacancies) and adsorption of hydroxyl (OH) groups on the zinc oxide surface. On the whole, the OI component prevails in the spectrum of the reference sample, but increasing the UV irradiation time leads to a redistribution in favor of the OII component. The redistribution is so significant that, in the case of sample *3* (the longest UV treatment time), there is only a signal from the higher energy component, which may be due to the high defect density on the ZnO surface. Generalized O 1*s* parameters according to the XPS data for the samples under investigation are presented in Table 3 together with the calculated percentages of the OI and OII species.

The approximate data in Table 3 and the spectra in Fig. 2 lead us to conclude that argon ion milling reduces the fraction of the OII species in all of the samples, which is attributable to the removal of the imperfect surface layer. At the same time, in the case of the samples synthesized using the sol–gel process adapted to flexible electronics, the higher energy component remains well-defined (its contribution is 63.62 at %) even after two-step cleaning. On the whole, this type of behavior of the OI and OII components cannot be accounted for by just the removal of hydroxyl (OH) groups from the surface. With allowance for our data on changes in atomic composition, it is reasonable to assume that there is an additional mechanism of ZnO film structure formation under UV irradiation. The final result of this process is the completion of surface structure formation and enrichment of the zinc oxide surface in oxygen with a binding energy of ~532.0 eV.

Table 3. O 1*s* parameters according to the XPS data for the samples differing in UV irradiation time

UV irradiation time, min	Binding energy, eV/concentration, at %					
	0		1		2	
	OI	OII	OI	OII	OI	OII
0	530.69/59.71	532.09/40.29	530.42/77.24	531.98/22.76	530.52/82.59	532.32/17.41
90	530.47/31.82	531.93/68.18	530.32/63.04	532.04/36.96	530.02/62.39	531.85/37.61
150	–/–	531.49/100	530.11/26.73	531.91/73.27	530.28/36.38	531.99/63.62

0, 1, and 2 have the same meaning as in Table 1.

Table 4. C 1*s* parameters according to the XPS data for the samples differing in UV irradiation time

UV irradiation time, min	Binding energy, eV/concentration, at %					
	0		1		2	
	CI	CII	CI	CII	CI	CII
0	285.28/90.44	288.99/9.56	285.08/82.03	289.26/17.97	285.08/74.74	289.07/25.26
90	285.21/70.50	288.71/29.50	285.39/71.81	289.12/28.19	284.85/82.08	288.84/17.92
150	284.5/81.98	288.41/18.02	285.35/78.46	289.03/21.54	284.77/74.31	288.02/25.69

0, 1, and 2 have the same meaning as in Table 1.

Specific features of the C 1*s* core level in the ZnO films. In the context of the above assumption, it appears also reasonable to analyze in detail the C 1*s* core level. Figure 3 shows C 1*s* spectra of the films before and after two-step surface cleaning. The spectra in Figs. 3a–3c correspond to the samples before Ar^+ ion etching; the spectra in Figs. 3d–3f were obtained after the first etching step; and the spectra in Figs. 3g–3i, after the second etching step. In the binding energy range under consideration (275–300 eV), there are well-defined peaks centered at 285.0 (CI) and 289.0 eV (CII). The former peak is most likely due to carbon in the form of pyrolytic graphite, and the latter, to an O=C–O group bonded to Zn atoms [14, 18, 19]. On the whole, these adsorbed carbon species are characteristic of all three samples. Note that the zinc oxide films produced using UV irradiation are characterized by a larger CII : CI atomic ratio and a shift of the peak to lower energies (≈0.5 eV for the samples before surface cleaning and ≈1 eV after two-step etching).

The mechanism underlying the formation of the groups under consideration during low-temperature heating (≈333 K) is not fully clear, but most likely it involves photoactivation processes, including photocatalytic oxidation and ozonation, which lead to partial decomposition of the organic components of the film-forming sol in air [20]. Generalized C 1*s* parameters according to the XPS data for the samples under investigation are presented in Table 4 together with the calculated percentages of the CI and CII species.

Ar^+ ion etching of the ZnO film surface leads to a redistribution of the atomic percentages of the CI and CII species. As a result, the fraction of the CII species in samples *1* and *3* increases, whereas the zinc oxide synthesized under UV irradiation for 90 min is characterized by opposite behavior: the fraction of CI increases from 70.50 to 71.81 and 83.08 at % after the first and second etching steps, respectively. This finding, the atomic compositions in Table 1, and similar behavior of the O 1*s* peak (Fig. 2), demonstrating that the OII species prevails over OI, lead us to conclude that sample *2* is intermediate between the samples prepared by the classic and adapted sol–gel processes. This in turn suggests that the structure formation processes in the ZnO films do not reach completion even upon UV treatment for 90 min. At the same time, it is reasonable to expect that raising the low-temperature annealing temperature will make it possible to speed up completion of ZnO structure formation.

Mechanism of structure formation of ZnO films in sol–gel nanosystems under UV irradiation. A generalized analysis of the present XPS data leads us to assume that the structure formation process in ZnO films comprises three main processes:

1. High-energy photons cause photochemical cleavage of alkoxy groups and activation of metal and oxygen atoms, facilitating the formation of Zn–O–Zn networks.

2. Interaction of UV radiation with atmospheric oxygen leads to the formation of ozone molecules, which in turn react with zinc oxide, enriching its surface with adsorbed oxygen and forming a zinc-deficient solid solution.

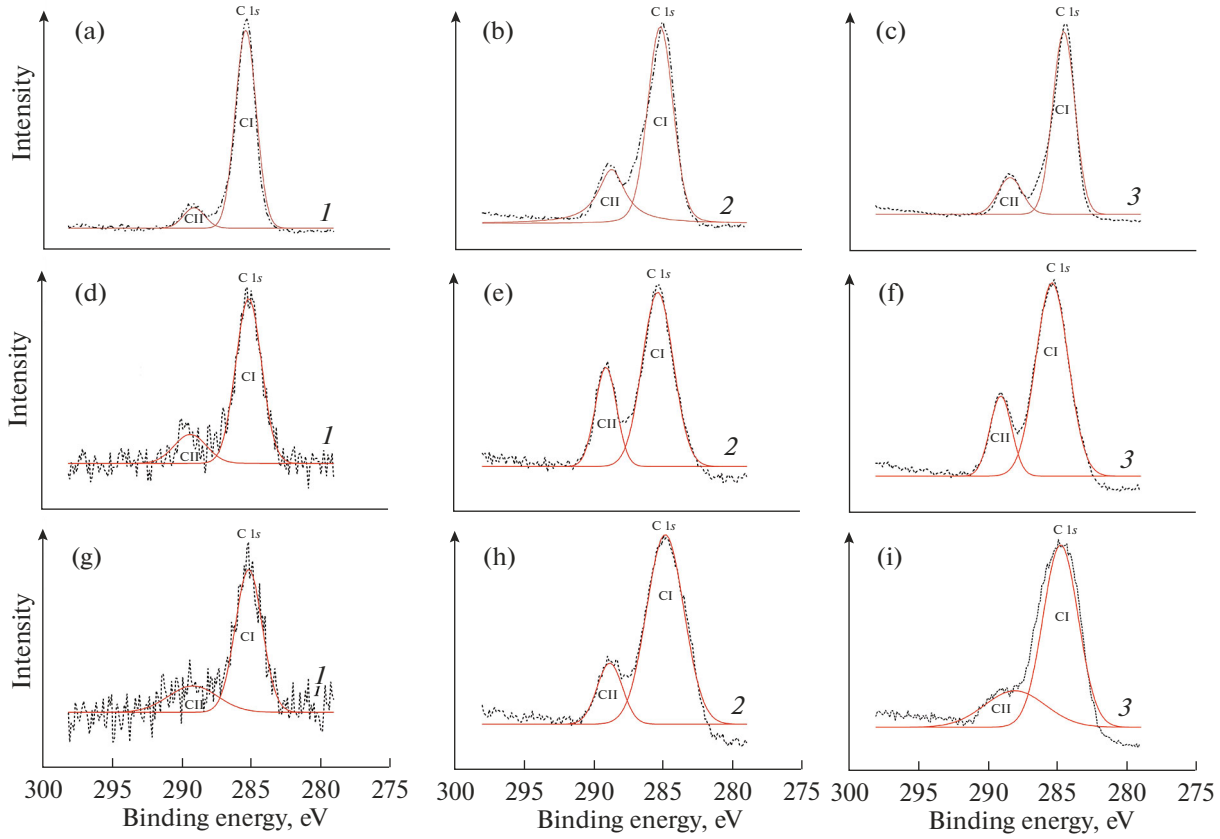

Fig. 3. C 1*s* spectra of the ZnO films produced at various UV photoannealing times: (a, d, g) high-temperature annealing, (b, e, h) UV photoannealing for 90 min, (c, f, i) UV photoannealing for 150 min; (b, e, h) first and (c, f, i) second Ar^+ etching steps.

3. The residual organics of the film-forming sol oxidizes by reacting with oxygen and considerably more reactive ozone.

The first and third processes play an advantageous role from the viewpoint of the formation of ZnO films suitable for flexible electronics, whereas the second process is negative. It leads to appreciable nonstoichiometry of the zinc oxide surface and carbon accumulation in the bulk of the film because adsorbed oxygen prevents complete desorption of organic components of the sol–gel nanosystem.

CONCLUSIONS

Using XPS, we have analyzed in detail zinc oxide structure formation in sol–gel nanosystems under UV irradiation. Based on survey core level spectroscopy results, we assessed the effect of UV irradiation time on the percentages of Zn, O, and C atoms in the films. Specific features of the O 1*s* and C 1*s* core levels have been analyzed before and after two-step Ar^+ ion etching of the film surface.

The observed decomposition of characteristic peaks into lower and higher energy components—OI (530.5 eV) + OII (532.0 eV) and CI (285.0 eV) + CII (289.0 eV)—and variations in their concentrations suggest that there is an additional mechanism of zinc oxide structure formation. The final result of photoactivation processes in the sol–gel nanosystem studied is the completion of surface structure formation and enrichment of the ZnO surface in oxygen with a binding energy of 532.0 eV, resulting in a zinc-deficient solid solution.

On the whole, the present results can be of interest for controlled synthesis of nanomaterials based on wide-band-gap metal oxides for purposes of flexible electronics.

ACKNOWLEDGMENTS

In this study, we used equipment at the Resource Centre for Physical Surface Characterization Methods, Research Park, St. Petersburg State University.

FUNDING

This work was supported by the Russian Federation President's Grant Council (State Support to Young Scientists of Russia and State Support to the Leading Scientific

Schools of the Russian Federation Programs, project nos. MD-172.2021.4, SP-3720.2021.1, and MK-3541.2021.1.2).

The elemental analysis of ZnO was supported by the Russian Foundation for Basic Research, grant no. 20-03-00026.

CONFLICT OF INTEREST

The authors declare that they have no conflicts of interest.

REFERENCES

1. Yu, K.J., Yan, Z., Han, M., and Rogers, J.A., Inorganic semiconducting materials for flexible and stretchable electronics, *NPJ Flexible Electron.,* 2017, vol. 1, no. 1, pp. 1–14. https://doi.org/10.1038/s41528-017-0003-z
2. Park, S., Park, H., Seong, S., and Chung, Y., Multilayer substrate to use brittle materials in flexible electronics, *Sci. Rep.,* 2020, vol. 10, no. 1, pp. 1–8. https://doi.org/10.1109/TED.2017.2647964
3. Thejaswini, H.C., Agasanapura, B., and Hopwood, J., Deposition and characterization of ZnO films using microplasma at atmospheric pressure, *Thin Solid Films,* 2016, vol. 603, pp. 328–333. https://doi.org/10.1016/j.tsf.2016.02.048
4. Son, D.I., Kwon, B.W., Park, D.H., Seo, W.S., Yi, Y., Angadi, B., Lee, C.L., and Choi, W.K., Emissive ZnO–graphene quantum dots for white-light-emitting diodes, *Nat. Nanotechnol.,* 2012, vol. 7, no. 7, p. 465. https://doi.org/10.1038/nnano.2012.71
5. Dimitrov, D.T., Nikolaev, N.K., Papazova, K.I., Krasteva, L.K., Pronin, I.A., Averin, I.A., Bojinova, A.S., Georgieva, A.Ts., Yakushova, N.D., Peshkova, T.V., Karmanov, A.A., Kaneva, N.V., and Moshnikov, V.A., Investigation of the electrical and ethanol-vapour sensing properties of the junctions based on ZnO nanostructured thin film doped with copper, *Appl. Surf. Sci.,* 2017, vol. 392, pp. 95–108. https://doi.org/10.1016/j.apsusc.2016.08.049
6. Tekin, D., Tekin, T., and Kiziltas, H., Photocatalytic degradation kinetics of orange G dye over ZnO and Ag/ZnO thin film catalysts, *Sci. Rep.,* 2019, vol. 9, no. 1, pp. 1–7. https://doi.org/10.1038/s41598-019-54142-w
7. Buonsanti, R., Llordes, A., Aloni, S., Helms, B.A., and Milliron, D.J., Tunable infrared absorption and visible transparency of colloidal aluminum-doped zinc oxide nanocrystals, *Nano Lett.,* 2011, vol. 11, no. 11, pp. 4706–4710. https://doi.org/10.1021/nl203030f
8. Lee, S.M., Kwon, J.H., Kwon, S., and Choi, K.C., A review of flexible OLEDs toward highly durable unusual displays, *IEEE Trans. Electron. Devices,* 2017, vol. 64, no. 5, pp. 1922–1931. https://doi.org/10.1109/TED.2017.2647964
9. Pronin, I.A., Averin, I.A., Yakushova, N.D., Karmanov, A.A., Moshnikov, V.A., and Terukov, E.I., Directional self-assembly of zinc oxide micro-and nanowires, *Tech. Phys. Lett.,* 2019, vol. 45, no. 6, pp. 628–631. https://doi.org/10.1134/S1063785019060282
10. Znaidi, L., Sol–gel-deposited ZnO thin films: a review, *Mater. Sci. Eng., B,* 2010, vol. 174, nos. 1–3, pp. 18–30. https://doi.org/10.1016/j.mseb.2010.07.001
11. Averin, I.A., Pronin, I.A., Yakushova, N.D., Karmanov, A.A., Alimova, E.A., Igoshina, S.E., Moshnikov, V.A., and Terukov, E.I., Sol–gel technology adaptation of nanostructured zinc oxide for flexible electronics, *Tech. Phys.,* 2019, vol. 64, no. 12, pp. 1821–1826. https://doi.org/10.1134/S1063784219120028
12. Han, W., Kim, J., and Park, H.H., Control of electrical conductivity of highly stacked zinc oxide nanocrystals by ultraviolet treatment, *Sci. Rep.,* 2019, vol. 9, no. 1, pp. 1–9. https://doi.org/10.1038/s41598-019-42102-3
13. Pronin, I.A., Yakushova, N.D., Averin, I.A., Karmanov, A.A., Moshnikov, V.A., and Dimitrov, D.Ts., Development of a physical model of thermovoltaic effects in the thin films of zinc oxide doped with transition metals, *Coatings,* 2018, vol. 8, no. 12, p. 433. https://doi.org/10.3390/coatings8120433
14. Komolov, A., Schaumburg, K., Møller, P.J., and Monakhov, V., Characterization of conducting molecular films on silicon: Auger electron spectroscopy, X-ray photoelectron spectroscopy, atomic force microscopy and surface photovoltage, *Appl. Surf. Sci.,* 1999, vol. 142, nos. 1–4, pp. 591–597. https://doi.org/10.1016/S0169-4332(98)00924-6
15. Li, L., Fang, L., Zhou, X.J., Liu, Z.Y., Zhao, L., and Jiang, S., X-ray photoelectron spectroscopy study and thermoelectric properties of Al-doped ZnO thin films, *J. Electron. Spectrosc. Relat. Phenom.,* 2009, vol. 173, no. 1, pp. 7–11. https://doi.org/10.1016/j.elspec.2009.03.001
16. Pronin, I.A., Averin, I.A., Karmanov, A.A., Yakushova, N.D., Komolov, A.S., Lazneva, E.F., Sychev, M.M., Moshnikov, V.A., and Korotcenkov, G., Control over the surface properties of zinc oxide powders via combining mechanical, electron beam, and thermal processing, *Nanomaterials,* 2022, vol. 12, no. 11, p. 1924. https://doi.org/10.3390/nano12111924
17. Pronin, I.A., Yakushova, N.D., Sychev, M.M., Komolov, A.S., Myakin, S.V., Karmanov, A.A., Averin, I.A., and Moshnikov, V.A., Evolution of acid–base properties of the surface of zinc oxide powders obtained by the method of grinding in an attritor, *Glass Phys. Chem.,* 2018, vol. 44, no. 5, pp. 464–473. https://doi.org/10.1134/S1087659618050140
18. Brinzari, V., Cho, B.K., and Korotcenkov, G., Carbon 1*s* photoemission line analysis of C-based adsorbate on (111) In_2O_3 surface: the influence of reducing and oxidizing conditions, *Appl. Surf. Sci.,* 2016, vol. 390, pp. 897–902. https://doi.org/10.1016/j.apsusc.2016.08.142
19. Komolov, A.S., Lazneva, E.F., Gerasimova, N.B., Panina, Yu.A., Baramygin, A.V., Zashikhin, G.D., and Pshenichnyuk, S.A., Structure of vacant electronic states of an oxidized germanium surface upon deposition of perylene tetracarboxylic dianhydride films, *Phys. Solid State,* 2016, vol. 58, no. 2, pp. 377–381. https://doi.org/10.1134/S106378341602013X
20. Kumar, B.G., Singh, R.P., and Nakamura, T., Degradation of carbon fiber-reinforced epoxy composites by ultraviolet radiation and condensation, *J. Compos. Mater.,* 2002, vol. 36, no. 24, pp. 2713–2733. https://doi.org/10.1177/002199802761675

Translated by O. Tsarev